Theoretical Studies of the Reaction Channels on the SO 2 /OH/NO Singlet Potential Energy Surface

ARTICLE *in* THE JOURNAL OF PHYSICAL CHEMISTRY A · MAY 2007

Impact Factor: 2.69 · DOI: 10.1021/jp067438r · Source: PubMed

2 AUTHORS:

Maria Wierzejewska
University of Wroclaw
61 PUBLICATIONS **474** CITATIONS
SEE PROFILE

Adriana Olbert-Majkut
University of Wroclaw
33 PUBLICATIONS **222** CITATIONS
SEE PROFILE

Theoretical Studies of the Reaction Channels on the SO_2/OH/NO Singlet Potential Energy Surface

Maria Wierzejewska* and Adriana Olbert-Majkut

Faculty of Chemistry, University of Wrocław, Joliot-Curie 14, 50-383 Wrocław, Poland

Received: November 10, 2006; In Final Form: February 16, 2007

Ab initio MP2/6-311++G(2d,2p) investigation of the SO_2/OH/NO singlet potential energy surface (PES) has been performed with the aim to localize and describe the existing minima and transition states linking them. The systematic studies have revealed seven minima, with the *trans*-HONO−SO_2 complex (**1t**) being the global minimum. Eight transition states between minima or between minima and the relevant reactant species have been described. Several available izomerization and dissociation routes have been identified and discussed. The most favorable association of $HOSO_2$ and NO was found to be a barrierless process forming nitrososulfonic acids. Isomerizations between trans-, cis-, and gauche- nitrososulfonic acids (**2t**, **2c**, and **2g**) are possible with low-energy barriers. The $HOSO_2$ and NO species can also react via another channels involving high-energy transition states to produce the HOSO−NO_2 (**3**) and HNO−SO_3 (**4**) complexes.

1. Introduction

Sulfur dioxide SO_2 and both OH and NO radicals are atmospheric species which chemistry and intermolecular interactions are of particular interest both for air pollution and combustion processes. Nitric oxide, NO, is an important primary pollutant emitted by both mobile and stationary sources. The combustion of sulfur containing fuels always yields SO_2 as a predominant sulfur containing pollutant. The OH radical is formed in polluted air directly from HONO and H_2O_2 photolysis:

$$HONO + h\nu \rightarrow OH + NO \quad (1.1)$$

$$H_2O_2 + h\nu \rightarrow 2OH \quad (1.2)$$

Under more polluted conditions, OH radicals are produced by photolysis of the products of incomplete combustion of fossil fuels such as aldehydes or ketones.[1]

The reaction of OH with SO_2 to form hydroxysulfonyl radical

$$OH + SO_2\,(+M) \rightarrow HOSO_2\,(+M) \quad (1.3)$$

is the first step in the gas-phase oxidation of sulfur dioxide into sulfuric acid[2] and has been recognized to be the major rate-controlling step in this process. Since early reports published by Cox[3] on photolysis of gaseous HONO/SO_2 system many papers appeared on kinetics of the above reaction using both experimental and theoretical techniques.[4−14]

Although NO is not expected to react directly with SO_2, it was suggested on the basis of experimental and theoretical considerations[15,16] that the predominant fate of $HOSO_2$ radical is reaction with O_2 forming $HOSO_2O_2$. This adduct may further react with NO according to the following reactions:

$$HOSO_2O_2 + NO \rightarrow HOSO_2O + NO_2 \quad (1.4)$$

$$HOSO_2O + NO \rightarrow HOSO_2ONO \quad (1.5)$$

The oxidation of NO and SO_2 is of great interest for the flue gas pollution control. Flue gas includes NO, SO_2, and O_2. If some OH or HO_2 radicals are present, the chain reactions may occur and the simultaneous oxidation of both pollutants takes place.[17]

The present paper reports a theoretical study of the SO_2/OH/NO singlet MP2/6-311++G(2d,2p) potential energy surface. Minima and transition states (TS) on the studied PES have been localized and characterized. Different reaction pathways resulting from interaction between the species of interest have been discussed. This subject is attractive because of its relevance to the atmospheric chemistry and the fact that the experimental evidence of a new compound, nitrososulfonic acid HO(NO)-SO_2, formed in low-temperature matrices have been recently reported.[18]

2. Computational Methods

All calculations were performed with the Gaussian 03 program package.[19] Structures of the minima, transition states (TS) and related monomers have been optimized at the MP2/6-311++G(2d,2p) level. Structural details for the species considered, not included below, are available as Supporting Information.

Minima and transition states were verified by calculation of vibrational frequencies. Minima were connected to each TS by following intrinsic reaction coordinate (IRC) generated at the MP2/6-311++G(2d,2p) level. To confirm that some addition or dissociation processes proceed without energy barrier, the potential energy surface scans have been performed at B3LYP/6-311++G(2d,2p) level. These results are included in Supporting Information.

Binding energies of the intermolecular complexes were corrected for the zero-point energies and for the basis set superposition error (with the exception of HOSO−NO_2 complex) using the counterpoise technique.[20]

The open-shell monomers have been treated by both unrestricted and restricted open shell methodology. As a check for the presence of spin contamination we used the value of the

* Corresponding author. Fax: (48)713282347. E-mail: mariaw@wchuwr.chem.uni.wroc.pl.

10.1021/jp067438r CCC: $37.00
Published on Web 03/21/2007

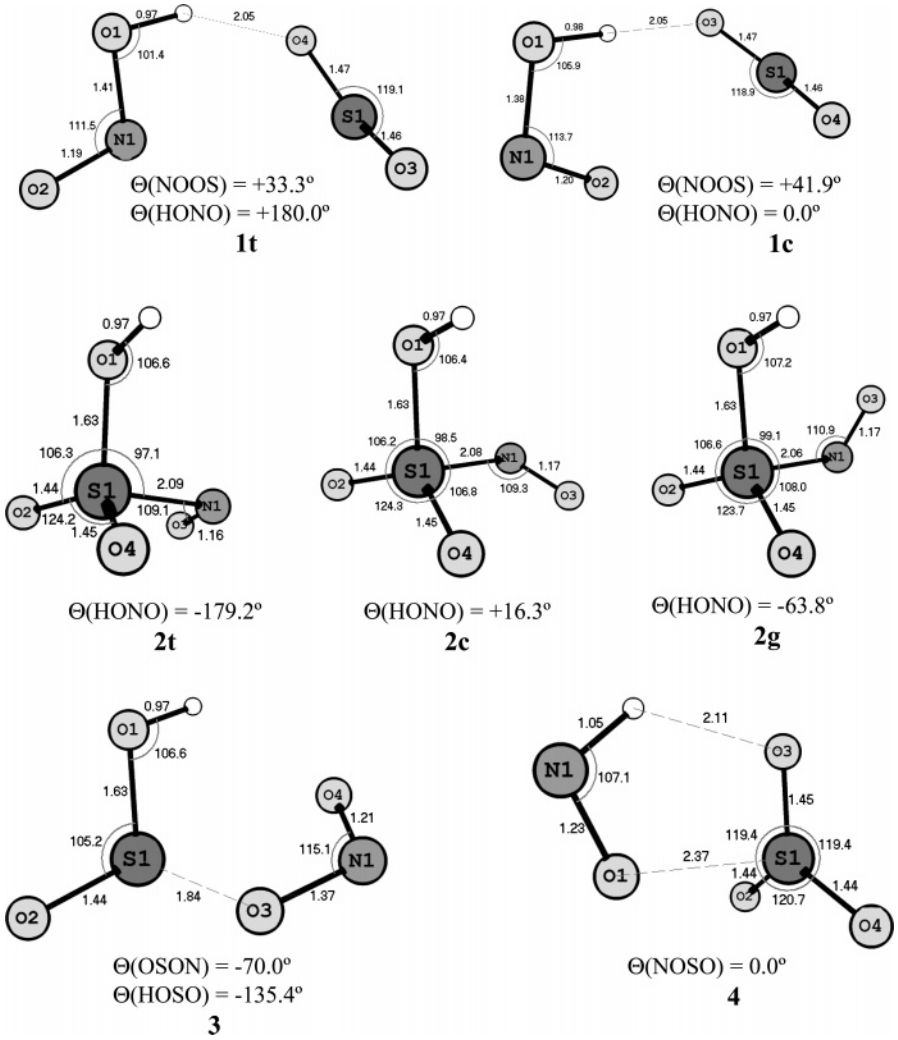

Figure 1. Optimized structure of the minima on the SO_2/OH/NO singlet potential energy surface.

total spin, $\langle S^2 \rangle$ which was found to differ only by 0.73−1.75% from the value of this parameter with no spin contamination. From now on the structures of the $HOSO_2$, HOSO, NO, and NO_2 species and the relevant energetics are those from the unrestricted MP2 calculations.

The topological analysis of the electron density (AIM) has been performed at the MP2/6-311++G(2d,2p) level using the AIM program as implemented in Gaussian 03. Bader's theory of "atoms in molecules" (AIM)[21] provides a rigorous and unambiguous criteria for the classification of the bonding in a molecular system. Two atoms are bonded if there is a bond path (BP) between their nuclei. The crucial element of the AIM analysis is finding critical points (BCP) of the electron density where $\nabla\rho(r_c) = 0$. Topological parameters derived from Bader's theory such as the electron density $\rho(r_c)$ and its Laplacian $\nabla^2\rho(r_c)$ at bond critical point allow to distinguish between two types of interactions. Covalent ("shared") interactions are characterized by a high value of the charge density at the BCP ($\rho(r_c) > 10^{-1}$au) and usually negative Laplacian. "Closed-shell" interaction present in ionic, hydrogen-bonded systems and van der Waals complexes show rather small $\rho(r_c)$ at BCP ($\leq 10^{-2}$ au) and positive Laplacian.[22]

3. Results and Discussion

The optimized geometry of minima localized on the SO_2/OH/NO potential energy surface at MP2/6-311++G(2d,2p) level are presented in Figure 1. The located transition states connecting the minima are displayed in Figure 2. The related energetics for both minima and transition states as well as for the relevant monomers is gathered in Table 1. The relative energies discussed in this chapter are those corrected for zero-point vibrational energy (ZPE).

The results of the AIM analysis performed in this paper are presented in Table 2 and the vibrational properties of the studied minima are given in Table 3. Figure 3 illustrates the potential energy diagram for the possible reaction pathways on the SO_2/OH/NO surface.

3.1. HONO−SO_2 Complexes (1t and 1c). While exploring the SO_2/OH/NO potential energy surface at MP2/ 6-311++G-(2d,2p) level two complexes formed between nitrous acid (HONO) and sulfur dioxide have been localized. Both *trans*- and *cis*-HONO isomers form hydrogen-bonded structures with the OH group interacting with one of the O atoms of the SO_2 molecule (**1t** and **1c**, respectively). These structures have been reported to be present in low temperature argon matrices and were earlier found on the MP2/6-31G(d) potential energy surface.[23] According to the present calculations the *trans*-HONO−SO_2 (**1t**) complex appeared to be a global minimum on the singlet SO_2/OH/NO PES with the cis-HONO−SO_2 (**1c**) being 0.94 kcal/mol higher in energy.

3.2. *trans*-HONO−SO_2 (1t) ↔ *cis*-HONO−SO_2 (1c) Isomerization. *trans*-HONO−SO_2 complex (**1t**) can rearrange endothermically to form the corresponding *cis*-HONO−SO_2 complex (**1c**) via TS_{1t-1c}. The TS_{1t-1c} transition state is

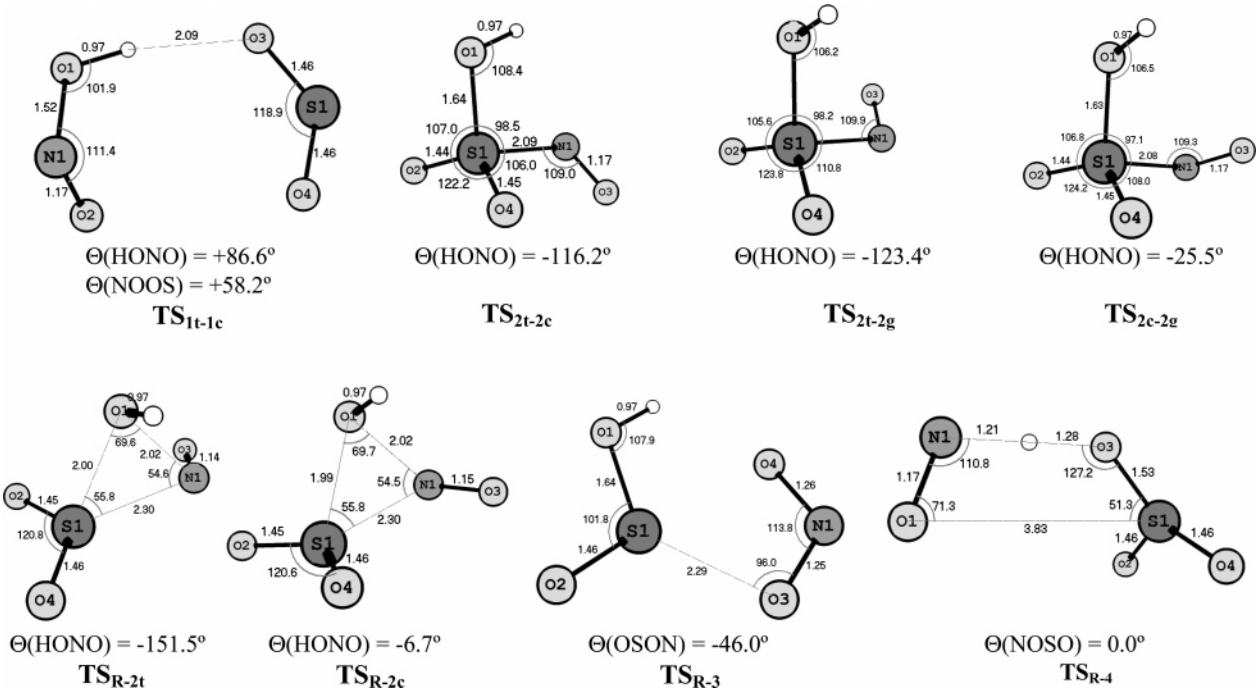

Figure 2. Optimized structure of the transition states on the SO_2/OH/NO singlet potential energy surface.

TABLE 1: Energies (in hartree) and Relative Energies (in kcal/mol) Calculated for Various Species on the SO_2/OH/NO Singlet Potential Energy Surface

species		energy (hartree)	ZPE (kcal/mol)	ΔE (kcal/mol)	$\Delta E + \Delta E_{ZPE}$ (kcal/mol)
		Minima			
trans-HONO−SO_2	1t	−753.20405054771	17.53	0.0	0.0
cis-HONO−SO_2	1c	−753.20248323772	17.49	0.98	0.94
t-HO(NO)SO_2	2t	−753.18166142587	18.29	14.05	14.81
c-HO(NO)SO_2	2c	−753.18062852130	18.27	14.70	15.44
g-HO(NO)SO_2	2g	−753.18016386349	18.27	14.99	15.73
HOSO−NO_2	3	−753.16866686154	17.85	22.20	22.52
HNO−SO_3	4	−753.16434020968	18.56	24.92	25.95
		Transition States			
TS_{1t-1c}	488i	−753.18476217366	15.80	12.10	10.37
TS_{2t-2c}	396i	−753.17238654064	17.64	19.87	19.98
TS_{2t-2g}	80i	−753.17880017356	18.11	15.84	16.42
TS_{2c-2g}	70i	−753.1794755117	18.12	15.42	16.01
TS_{R-2t}	373i	−753.15765597120	17.22	29.11	28.80
TS_{R-2c}	397i	−753.15396386226	17.19	31.43	31.09
TS_{R-3}	251i	−753.14663056656	17.78	36.03	36.28
TS_{R-4}	2711i	−753.10805270391	14.32	60.24	57.03
		Monomers[a]			
$HOSO_2$		−623.49967432	14.16		
trans-HONO		−205.33456140098	12.41		
cis-HONO		−205.33356981158	12.48		
SO_2		−547.86205598342	4.09		
SO_3		−622.92064561694	7.50		
HNO		−130.22979758788	8.72		
cis-HOSO		−548.42610955	10.60		
trans-HOSO		−548.42141489	10.68		
NO_2		−204.71544575	6.87		
NO		−129. 65537789	4.87		

[a] For radical species projected UMP2 energy is given

characterized by a strongly elongated N−O bond in nitrous acid unit with the distance of 1.522 Å (1.413 Å in **1t** and 1.384 Å in **1c** complexes) and the HONO dihedral angle of 86.6°; the value intermediate between those found in *trans*-HONO−SO_2 and *cis*-HONO−SO_2 complexes (180.0° and 0.0°, respectively). The reaction coordinate involves the OH torsion with the imaginary frequency of 488i cm^{-1}. The calculated energy barrier for *trans*-HONO−SO_2 (**1t**) → *cis*-HONO−SO_2 (**1c**) process with respect to **1t** including zero-point correction equals to 10.37 kcal/mol. This result is in accordance with that reported in the literature for the *trans*-HONO → *cis*-HONO isomerization. The corresponding torsional barrier (corrected for ΔZPE) calculated for this process at different levels of theory ranges from 10.5 to 12.0 kcal/mol[24−26] while the experimental gas-phase values are between 11.6 and 12.1 kcal/mol.[27,28] It is also worth noting that the HONO dihedral angle calculated for the transition state between *trans*-HONO and *cis*-HONO conformers ranges

TABLE 2: Electron Density $\rho(r_c)$ and Laplacian of the Electron Density $\nabla^2\rho(r_c)$ (in au) for the Relevant Bond Critical Points (BCP) in the Studied Complexes

				HNO-SO_3 (**4**)	
BCP	t-HONO-SO_2 (**1t**) H···O	c-HONO-SO_2 (**1c**) H···O	HOSO-NO_2 (**3**) S···O	S···O	H···O
$\rho(r_c)$	0.0170	0.0180	0.1410	0.0442	0.0203
$2\rho(r_c)$	0.0695	0.0631	0.0223	0.1129	0.0744

TABLE 3: Unscaled Vibrational Frequencies (cm^{-1}) and Intensities (in Parentheses) ($kmmol^{-1}$) Calculated for the Minima and the Relevant Monomers

spec ies	
1t	37(5), 41(5), 52(1), 122(5), 135(9), 146(10), 496(27), 644(129), 697(77), 838(185), 1080(2 9), 1284(151), 1355(169), 1626(89), 3712(284)
1c	30(0), 48(2), 54(4), 121(4), 124(7), 137(11), 497(32), 651(29), 772(84), 919(328), 1078(29), 1283(141), 1363(10), 1586(117), 3572(262)
2t	78(2), 114(8), 174(22), 182(38), 309(77), 415(18), 439(17), 562(57), 630(27), 760(259), 1 136(43), 1159(195), 1389(227), 1666(486), 3782(144)
2c	73(2), 119(20), 174(8), 175(46), 306(45), 420(45), 439(21), 564(50), 632(16), 760(261), 1 132(38), 1163(195), 1391(227), 1652(472), 3781(131)
2g	61(1), 137(53), 164(3), 182(11), 318(53)423(42), 433(14), 567(63), 610(23), 783(204), 11 28(46), 1167(207), 1390(245), 1634(427), 3788(133)
3	113(5), 190(8), 212(10), 266(22), 300(114), 365(34), 441(81), 508(155), 758(113), 793(1 29), 897(271), 1128(140), 1300(147), 1489(126), 3728(98)
4	67(3), 151(21), 166(8), 196(1), 350(41), 474(135), 509(61), 518(20), 584(51), 1026(6), 13 53(203), 1386(177), 1482(5), 1602(47), 3122(4)
	Monomers
***trans*-HONO**	581(105), 582(221), 794(154), 1290(178), 1643(108), 3790(92)
***cis*-HONO**	620(53), 683(105), 869(367), 1329(8), 1596(142), 3635(40) SO_2 492(27), 1078(20), 1292(143)
***cis*-HOSO**	160(131), 370(25), 753(231), 1095(24), 1285(376), 3752(131) NO_2 767(5), 1352(1), 2685(8293) /757, 1300, 1802[a,b]
***trans*-HOSO**	114(108), 393(9), 735(163), 1081(126), 1364(437), 3787(111) NO 2685(1366)/1876[a,c]
HNO	1456(12), 1584(28), 3062(93) SO_3 475(26), 510(28), 510(28), 1020(0), 1366(169), 1366(169)

[a] Since frequencies and intensities calculated for the NO_2 and NO species with unrestricted formalism are poorly reproduced, the corresponding values obtained by restricted open shall MP2/6-311++G(2d,2p) are given after slash. [b] NO_2 frequencies in argon matrix: 1611.3, 1321.0 and 748.2 cm^{-1} [43]. [c] NO frequency in argon matrix: 1871.8 cm^{-1} [44].

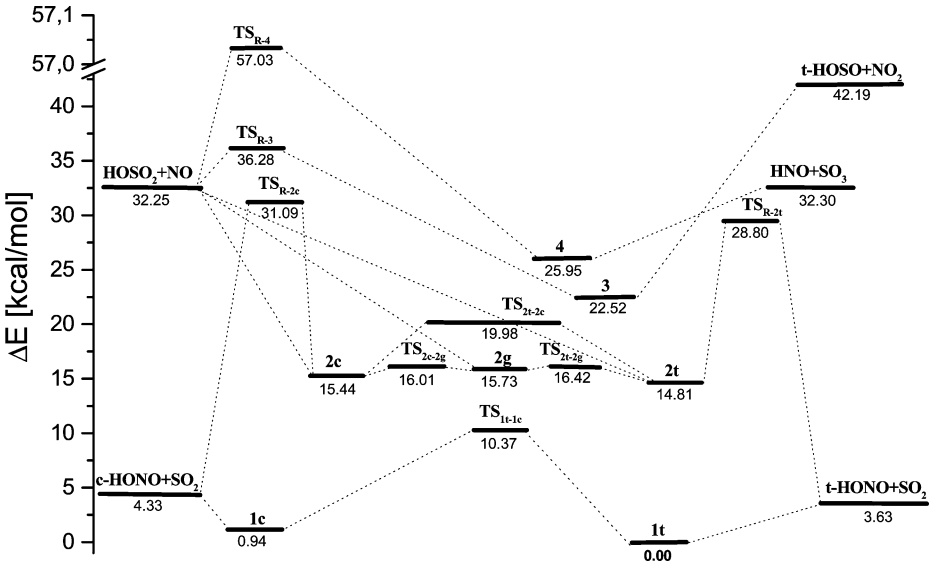

Figure 3. ZPE corrected MP2 potential energy diagram for the SO_2/OH/NO system.

between 85.4 and 86.9°[24] and compares well with that found for TS_{1t-1c} in this work.

3.3. Nitrososulfonic Acids (2t, 2c and 2g). As it has been recently reported, the UV photolysis of HONO−SO_2 complexes isolated in argon and nitrogen matrices leads to the formation of the nitrososulfonic acid HO(NO)SO_2 molecule. The cis and trans isomers of this species have been described theoretically, and it was suggested on the basis of the infrared spectra that both of them might be isolated in the studied low-temperature matrices.[18] The present calculations reveal the existence of a third isomer of nitrososulfonic acid which possesses a gauche conformation. The optimized structures of three isomers trans-, cis- and gauche-nitrososulfonic acid (**2t, 2c**, and **2g)** are presented in Figure 1. Three conformers differ by the relative position of the OH and NO groups and are characterized by the Θ (HONO) dihedral angle equal to −179.2°, 16.3°, and −63.8°, for **2t, 2c**, and **2g**, respectively. The trans-, cis- and gauche-nitrososulfonic acids lie 14.81, 15.44, and 15.73 kcal/mol above the global minimum **1t**, respectively, while the energy separation between three conformers is less than 1 kcal/mol.

As Figure 3 shows, the trans- and cis-nitrososulfonic acids can be formed from the *trans*-HONO or *cis*-HONO and SO_2 reactants. The processes proceed via product-like transition states TS_{R-2t} and TS_{R-2c} laying 28.80 and 31.09 kcal/mol, respectively, above the global minimum. These transition states differ by the relative orientation of OH and NO moieties in analogy to their position in **2t** and **2c**. The imaginary frequencies of 373i and 397i in TS_{R-2t} and TS_{R-2c} correspond to the complex motion of S and N atoms and the O−H moiety.

3.4. Isomerizations between trans-, cis- and gauche-Nitrososulfonic Acids. The least stable gauche conformer **2g** may easily isomerize to form more stable **2t** or **2c**. The isomerizations proceed with very low-energy barriers of 0.32−1.61 kcal/mol through TS_{2t-2g} and TS_{2c-2g}, respectively. These transition states, laying 16.42 and 16.01 kcal/mol higher than the global minimum, are characterized by the dihedral angles Θ(HONO) of −123.4° and −25.5° which are the intermediate values as compared to those observed for the corresponding minima **2t** and **2g** or **2c** and **2g**. Both **2g** ↔ **2t** and **2g** ↔ **2c** isomerizations proceed through the NO torsion characterized by relatively low imaginary frequency of 80i and 70i cm^{-1}, respectively.

In turn, the direct isomerization between trans- and cis-nitrososulfonic acids (**2t** ↔ **2c**) proceeds through the higher energy TS_{2t-2c} lying 19.98 kcal/mol above the global minimum. This transition state is characterized by the Θ(HONO) of −116.2° and the imaginary frequency of 396i cm^{-1} corresponding to the OH torsion as a reaction coordinate. The calculated energy barrier for the direct **2t** → **2c** isomerization equals to 5.17 kcal/mol and is slightly higher than those obtained for **2g** ↔ **2t** and **2g** ↔ **2c** processes. The relatively low-energy barriers for the isomerizations between trans-, cis- and gauche-nitrososulfonic acids predicted by the present calculations confirm the suggestion[18] that different conformers of nitrososulfonic acid might be produced in argon matrices after photolysis of the $HONO/SO_2$/Ar system.

3.5. HOSO−NO_2 (3) HNO−SO_3 (4) Complexes. Two other minima localized on the SO_2/OH/NO PES, namely, HOSO−NO_2 (**3**) and HNO−SO_3 (**4**) complexes lie significantly higher as compared to the remaining minima and are situated 22.52 and 25.95 kcal/mol above the global minimum **1t,** respectively. As presented in Figure 1, these complexes are arranged in such a way that both hydrogen-bonded and van der Waals interaction are possible. In order to detect the existence of H-bond or/and S···O noncovalent interaction in **3** and **4**, we performed the atoms in molecules (AIM) calculations.[21] Table 2 shows the topological parameters derived from the Bader's theory such as electron density $\rho(r_c)$ and its Laplacian $\nabla^2\rho(r_c)$ at the H...O or S...O bond critical points (BCP) for the HOSO−NO_2 (**3**) and HNO−SO_3 (**4**) complexes. For comparison purposes the results obtained for the HONO−SO_2 complexes (**1t**, **1c**) are also given. It is evident that in the HOSO−NO_2 adduct (**3**), there is the bond path connecting S atom with one of the O atoms of nitrogen dioxide while the H...O contact does not exist. In turn, for HNO−SO_3 (**4**) both H···O hydrogen bond and S···O interaction have been detected. Topological criteria require the electron density and its Laplacian to be in the proper range of 0.002−0.04 and 0.02−0.15 au, respectively, for hydrogen bonding[22] and similar small positive values for these parameters are expected for Van der Waals complexes. These conditions are fulfilled with one exception of the $\rho(r_c)$ value obtained for the S···O bond in the HOSO−NO_2 adduct. This parameter in **3** is higher than expected and together with the calculated relatively short S···O distance of 1.843 Å indicates a very strong intermolecular interaction. This conclusion is in line with a high value of the calculated binding energy for HOSO−NO_2 reported in section 3.7.

It is interesting to note that the HOSO subunit in the HOSO−NO_2 complex **3** possesses a planar trans conformation. In spite of many attempts, we failed to localize a minimum corresponding to the *cis*-HOSO−NO_2 complex. The HOSO radical itself was a subject of the extensive studies[29] at different levels of theory and it was concluded that the nonplanar *cis*-HOSO isomer is the most stable species while the planar *trans*-HOSO isomer was found to be a transition state. According to the present calculations performed for HOSO molecule, the obtained structure is strongly dependent on the formalism used. Using the restricted open-shell approach, only the cis conformer of C_1 symmetry was found to be a minimum. In turn, the unrestricted MP2/6-311++G(2d,2p) calculations give a planar structure for both cis- and trans-HOSO isomers with the former being more stable by ca. 2.9 kcal/mol. The present study revealed also that the *cis*-HOSO ↔ *trans*-HOSO process proceeds through a small isomerization barrier of ca. 3 kcal/mol. The transition state involved is nonplanar and is characterized by the dihedral angle of 135.4°. It is worth mentioning that the trans configuration of the HOSO radical has been recently found in the O_2−HOSO complex.[30]

Weak complexes formed between SO_3 and simple molecules as H_2O, HX or HOX have been extensively studied both experimentally and theoretically.[31−38] For SO_3−H_2O all papers report the structure with O···S interaction and with the eclipsed configuration of the subunits.[34] In turn, for SO_3−HF, SO_3−HCl, and SO_3−HBr complexes microwave[35] studies indicate that weakly bound adducts are formed with the proton in HF tilted away from SO_3, while those in HCl and HBr tilted toward it. The present calculations show that both H...O hydrogen bond and noncovalent interaction between S and O atoms are present in the HNO−SO_3 complex. The electronic density $\rho(r_c)$ found in H···O bond critical point is smaller than that found in the S···O bond critical point in spite of the fact that usually van der Waals complexes present electronic density values closer to 10^{-3} au while for hydrogen-bonded species the values are in the range of 10^{-2} au.[22,39] Thus, the H-bonding interaction seems to be of less importance for the stability of **4**. This observation is consistent with the results of the computational investigation reported for HOX−SO_3 (X═F, Cl, Br).[38] It is worth mentioning that the results of the vibrational frequencies calculations (Table 3) performed for the HNO−SO_3 complex reveal a blue shift of the N−H stretching mode in HNO−SO_3 dimer of 60 cm^{-1} as compared to the HNO monomer value. Such blue-shifted H-bonds well-known in the C−H···X systems have been recently reported for several complexes with HNO as a proton donor [40−42] and the HNO−SO_3 complex (**4**) may represent a new interesting example of the series.

3.6. Reactions between $HOSO_2$ and NO Radicals. Both hydroxysulfonyl radical $HOSO_2$ and nitrogen monoxide are the key species in atmospheric chemistry. It was interesting to follow possible reactions involving these two species, namely:

$$HOSO_2 + NO \rightarrow HOSO + NO_2 \qquad (3.6.1)$$

$$HOSO_2 + NO \rightarrow HNO + SO_3 \qquad (3.6.2)$$

The present calculations indicate that $HOSO_2$ and NO radicals may react according to the reaction 3.6.1 via the product-like transition state TS_{R-3} to form the HOSO...NO_2 complex (**3**). The calculated energy barrier for this process is relatively low and equals to 4.03 kcal/mol. In the next step the HOSO...NO_2

TABLE 4: Binding Energies (in kcal/mol) Calculated at MP2/6-311++G(2d,2p) Level for Different Complexes on the HO/NO/SO_2 Potential Energy Surface

complex		energy in kcal/mol[a] ΔE^{CP}	$\Delta E^{CP}{}_{ZPE}$
trans-HONO−SO_2	(**1t**)	−3.22	−2.19
cis-HONO−SO_2	(**1c**)	−2.85	−1.93
HOSO−NO_2	(**3**)	−19.96	−18.95
HNO−SO_3	(**4**)	−10.85	−8.51

[a] CP, basis set supperposition correction; ZPE, zero-point vibrational energy correction.

complex (**3**) disintegrates endothermically with a high-energy barrier of 19.67 kcal/mol to give product species HOSO and NO_2. According to our calculations another reaction channel is also possible for the $HOSO_2$ and NO species (reaction 3.6.2). As a first step the high-energy transition state $TS_{\mathbf{R-4\ is}}$ formed. It is located 57.03 kcal/mol above the global minimum. The $TS_{\mathbf{R-4}}$ shows C_s symmetry with the NO and SO_3 moieties sharing the H atom situated between N atom of NO and one of the O atoms of SO_3. The reaction proceeds through the proton motion characterized by the imaginary frequency of 2711i cm^{-1} leading to the hydrogen-bonded HNO−SO_3 complex (**4**). The $HOSO_2$ + NO → HNO−SO_3 process is predicted to be exothermic by 6.30 kcal/mol.

It is worth noting that according to our calculations both reactions (3.6.1 and 3.6.2) are not kinetically feasible at normal temperature due to the high-energy transition states above the reactants involved. In turn, a simple addition leading to the trans-, cis-, or gauche-nitrososulfonic acids is expected to be a barrierless process. Thus, the observation that simultaneous presence of $HOSO_2$ and NO radicals in low-temperature matrices[18] leads to the nitrososulfonic acids as only products is justified by the present calculations.

3.7. Binding Energies in the Studied Complexes. The BSSE and ZPE corrected binding energies for the studied complexes are given in Table 4. The values obtained for the complexes formed between trans- and cis-nitrous acid and sulfur dioxide are consistent with those reported earlier[23] and confirm rather weak interaction in **1t** and **1c**. For the HOSO−NO_2 complex, a much larger binding energy of −18.95 kcal/mol found at MP2/6-311++G(2d,2p) level seems to be justified by the fact that two radicals are involved in the interaction. The HNO−SO_3 complex with the binding energy of −8.51 kcal/mol is relatively strong as compared with **1t** and **1c.** As it was mentioned earlier, the results of AIM analysis point out to two types of interaction in **4**, both contributing to the overall stability of the complex. The value of −8.51 kcal/mol obtained for HNO−SO_3 may be compared with other SO_3 complexes. Solimannejad and Pejov[38] have recently reported the results of the MP2/6-311++G(2df,-2p) study performed for the HXO−SO_3 systems. The predicted binding energies (ZPE corrected) are equal to −4.07, −4.43, and −4.77 kcal/mol for X=F, Cl and Br, respectively.

4. Summary

The SO_2/OH/NO potential energy surface have been explored at MP2/ 6-311++G(2d,2p) level. Our calculations have revealed seven minima with the *trans*-HONO−SO_2 (**1t**) complex being the global minimum. Eight transition states between minima or between minima and the relevant reactant species have been described. Reaction of *trans*- and *cis*-HONO with SO_2 leads to the formation of hydrogen-bonded complexes **1t** and **1c** or proceeds via the high-energy transition states $TS_{\mathbf{R-2t}}$ and $TS_{\mathbf{R-2c}}$ producing nitrososulfonic acids (**2t**, **2c**). The hydroxysulfonyl radical $HOSO_2$ and nitrogen monoxide, the key species in atmospheric chemistry, may react via high-energy $TS_{\mathbf{R-3}}$ and $TS_{\mathbf{R-4}}$ to form HOSO−NO_2 (**3**) and HNO−SO_3 (**4**) complexes, respectively. More feasible reaction between $HOSO_2$ and NO is a barrierless addition forming three different isomers of nitrososulfonic acid (**2t**, **2c** and **2g**).

Acknowledgment. The authors thank Prof. Z. Latajka and dr M. Biczysko for helpful discussions. A grant of computer time from the Wrocław Center for Networking and Supercomputing is gratefully acknowledged. A.O−M. thanks the Foundation for Polish Science for financial support.

Supporting Information Available: Calculated geometry of the minima, transition states and monomers. Free energy differences for the species involved. Results of the PES scans for the barrierless processes. This material is available free of charge via Internet at http://pubs.acs.org.

References and Notes

(1) Hewitt, C. N. *Atmos. Environ.* **2001**, *35*, 1155.
(2) Stockwell, W. R.; Calvert, J. G. *Atmos. Environ*. **1983**, *17*, 2231.
(3) Cox, R. A. *J. Photochem*. **1974/75**, *3*, 291.
(4) Wine, P. H.; Thompson, R. J.; Ravishanakara, A. R.; Semmes, D. H.; Gump, C. A.; Torabi, A.; Nicovich, J. M. *J. Phys. Chem*. **1984**, *88*, 2095.
(5) Margitan, J. J. *J. Phys. Chem*. **1984**, *88*, 3314.
(6) Martin, D.; Jourdain, J. L.; Bras, G. L. *J. Phys. Chem*. **1986**, *90*, 4143.
(7) Lee, Y. -Y.; Kao, W. -C.; Lee, Y. -P. *J. Phys. Chem*. **1990**, *94*, 4535.
(8) Fulle, D.; Hamann, H. F.; Hippler, H. *Phys. Chem. Chem. Phys*. **1999**, *1*, 2695 and references cited therein.
(9) Lee, W.-K.; McKee, M. L. *J. Phys. Chem. A* **1997**, *101*, 9778.
(10) Leung, F.-Y.; Colussi, A. J.; Hoffmann, M. R. *J. Phys. Chem. A* **2001**, *105*, 8073.
(11) Moore-Plummer, P. L.; Wu, R.; Flenner, J. *J. Mol. Phys.* **2002**, *100*, 1847.
(12) Blitz, M. A.; Hughes, K. J.; Pilling, M. J. *J. Phys. Chem*. **2003**, *107*, 1971.
(13) Somnitz, H. *Phys. Chem. Chem. Phys*. **2004**, *6*, 3844.
(14) Somnitz, H.; Gleitsmann, G. G.; Zellner, R. *Meteorol. Z.* **2005**, *14*, 459.
(15) Davis, D. D.; Ravishankara, A. R.; Fischer, S. *Geophys. Res. Lett*. **1979**, *6*, 113.
(16) Majumdar, D.; Kim, G.-S.; Kim, J.; Oh, K. S.; Lee, J. Y.; Kim, K. S.; Choi, W. Y.; Lee, S.-H.; Kang, M.-H.; Mhin, B. J. *J. Chem. Phys*. **2000**, *112*, 723.
(17) Song, Q. *Energy & Fuels* **2003**, *17*, 1549.
(18) Wierzejewska, M.; Olbert-Majkut, A. *J. Phys. Chem. A* **2003**, *107*, 10944.
(19) Frisch, M. J.; Trucks, G. W.; Schlegel, H. B.; Scuseria, G. E.; Robb, M. A.; Cheeseman, J. R.; Montgomery, J. A., Jr.; Vreven, T.; Kudin, K. N.; Burant, J. C.; Millam, J. M.; Iyengar, S. S.; Tomasi, J.; Barone, V.; Mennucci, B.; Cossi, M.; Scalmani, G.; Rega, N.; Petersson, G. A.; Nakatsuji, H.; Hada, M.; Ehara, M.; Toyota, K.; Fukuda, R.; Hasegawa, J.; Ishida, M.; Nakajima, T.; Honda, Y.; Kitao, O.; Nakai, H.; Klene, M.; Li, X.; Knox, J. E.; Hratchian, H. P.; Cross, J. B.; Bakken, V.; Adamo, C.; Jaramillo, J.; Gomperts, R.; Stratmann, R. E.; Yazyev, O.; Austin, A. J.; Cammi, R.; Pomelli, C. W.; Ochterski, J.; Ayala, P. Y.; Morokuma, K.; Voth, G. A.; Salvador, P.; Dannenberg, J. J.; Zakrzewski, V. G.; Dapprich, S.; Daniels, A. D.; Strain, M. C.; Farkas, O.; Malick, D. K.; Rabuck, A. D.; Raghavachari, K.; Foresman, J. B.; Ortiz, J. V.; Cui, Q.; Baboul, A. G.; Clifford, S.; Cioslowski, J.; Stefanov, B. B.; Liu, G.; Liashenko, A.; Piskorz, P.; Komaromi, I.; Martin, R. L.; Fox, D. J.; Keith, T.; Al-Laham, M. A.; Peng, C. Y.; Nanayakkara, A.; Challacombe, M.; Gill, P. M. W.; Johnson, B.; Chen, W.; Wong, M. W.; Gonzalez, C.; Pople, J. A. *Gaussian 03*, Revision C.02; Gaussian, Inc.: Wallingford CT, 2004.
(20) Boys, S. F.; Bernardi, F. *Mol. Phys*. **1970**, *19*, 53.
(21) Bader, R. F. *Atoms In Molecules: A Quantum Theory*; Oxford University Press: New York, 1990.
(22) Koch, U.; Popelier, P. L. A. *J. Phys. Chem. A* **1995**, *99*, 9747.
(23) Wierzejewska, M.; Mielke, Z.; Wieczorek, R.; Latajka, Z. *Chem. Phys.* **1998**, *228*, 17.
(24) de Maré, G. R.; Moussaoui, Y. *Int. Rev. Phys. Chem*. **1999**, *18*, 91 and references cited therein.

(25) Bauerfeldt, G. F.; Arbilla, G.; da Silva, E. C. *J. Phys. Chem. A* **2000**, *104*, 10895.
(26) Luckhaus, D. *Chem. Phys.* **2004**, *304*, 79.
(27) Jones, L. H.; Badger, R. M.; Moore, G. E. *J. Chem. Phys*. **1951**, *19*, 1599.
(28) McGraw, G. E.; Bernitt, D. L.; Hisatsune, I. C. *J. Chem. Phys.* **1966**, *45*, 1392.
(29) Napolion, B.; Watts, J. D. *Chem. Phys. Lett.* **2006**, *421*, 562 and references cited therein.
(30) Wang, B.; Hou, H. *Chem. Phys. Lett*. **2005**, *410*, 235.
(31) Tso, T. -L.; Lee, E. K. C. *J. Phys. Chem*. **1984**, *88*, 2776.
(32) Bondybey, V. E.; English, J. H. *J. Mol. Spectrosc*. **1985**, *109*, 221.
(33) Schriver, L.; Carrere, D.; Schriver, A.; Jaeger, K. *Chem. Phys. Lett*. **1991**, *181*, 505.
(34) Standard, J. M.; Buckner, I. S.; Pulsifer, D. H. *J. Mol. Struct (THEOCHEM*) **2004**, *673*, 1.
(35) Phillips, J. A.; Canagaratna, M.; Goodfriend, H.; Leopold, K. R. *J. Phys. Chem.* **1995**, *99*, 501.
(36) Canagaratna, M.; Phillips, J. A.; Goodfriend, H.; Fiacco, D. L.; Ott, M. E.; Harms, B.; Leopold, K. R. *J. Mol. Spectrosc*. **1998**, *192*, 338.
(37) Weber, K. H.; Harries, J. A.; Larson, L. J.; Tao, F.-M. *J. Theor. Comp. Chem*. **2005**, *4*, 623.
(38) Solimannejad, M.; Pejov, L. *J. Phys. Chem. A* **2005**, *109*, 825.
(39) Oliveira, B. G.; Pereira, F. S.; de Araújo, R. C. M. U.; Ramos, M. N. *Chem. Phys. Lett.* **2006**, *427*, 181.
(40) Li, A. Y. *J. Phys. Chem. A* **2006**, *110*, 10805.
(41) Yang, Y.; Zhang, W. J.; Gao, X. M. *Int. J. Quantum Chem*. **2006**, *106*, 1199.
(42) Liu, Y.; Liu, W. Q.; Yang, Y.; Liu, J. G. *Int. J. Quantum Chem*. **2006**, *106*, 2122.
(43) Olbert-Majkut, A.; Mielke, Z.; Wieczorek, R.; Latajka, Z. *Int. J. Quantum Chem*. **2002**, *90*, 1140.
(44) Mielke, Z.; Latajka, Z.; Olbert-Majkut, A.; Wieczorek, R. *J. Phys. Chem. A* **2000**, *104*, 3764.